Proceedings of the 17th International Symposium on the Packaging and Transportation of Radioactive Materials
PATRAM 2013
August 18-23, 2013, San Francisco USA

LOADING ON FUEL RODS IN A SURROGATE PWR ASSEMBLY SUBJECTED TO SIMULATED NORMAL CONDITIONS OF TRUCK TRANSPORT

Paul McConnell
Sandia National Laboratories

Doug Ammerman
Sandia National Laboratories

Ken Sorenson
Sandia National Laboratories

ABSTRACT
Tests were performed to directly measure loads on fuel rods in a fuel assembly subjected to conditions of normal truck transport. A PWR assembly with surrogate fuel rods was subjected to vibration and shock spectra derived from data obtained by measuring accelerations on actual truck casks. The fuel assembly was within a basket which was attached to a shaker simulating the configuration of an assembly within a truck cask. Three Zircaloy-4 fuel rods were instrumented with accelerometers and strain gauges to measure the loads on the rods imparted by vibrations and shocks. The results are discussed in terms of potential implications of the transport of embrittled fuel-rod cladding.

INTRODUCTION
Long-term storage and subsequent transportation of high-burnup used nuclear fuel (UNF) is an issue requiring quantitative knowledge of UNF material properties and its response to mechanical loadings during transport. The fuel cladding is the first line of defense for containment of the used nuclear fuel; therefore, it is important to understand if cladding can maintain its integrity during normal conditions of transportation.
Normal conditions of transport are those defined within the United States Nuclear Regulatory Commission (NRC) regulations in 10 Code of Federal Regulations (CFR) Part 71 [1] and the International Atomic Energy Agency SSR-6 regulations [2]. The Part 71 regulations require packages for transporting UNF to meet certain conditions during normal transport. The effect of "vibration normally incident to transport" must be determined for a package design (§71.71(c)(5)). The NRC provides guidance in §2.5.6.5 *Vibration* in the "Standard Review Plan for Transportation Packages for Radioactive Material", NUREG-1609 [3], which cites NUREG/CR-0128 and NUREG/CR-1277 [4-5]. These documents include information on shock loadings and random vibration.

PURPOSE
This test program was designed to better understand fuel rod response to *normal* conditions of truck transport (NCT) loadings in order to estimate the ability of UNF to withstand these

conditions. The experimental work was focused on testing a 17×17 PWR assembly containing instrumented surrogate fuel rods placed upon a shaker to simulate vibrational and shock loading associated with a normal 700-mile truck journey.

The data from the tests described herein shall be compared to data to be generated in other DOE Used Nuclear Fuel Disposition Campaign separate effects testing activities which will measure mechanical properties of high-burnup and aged UNF. Comparing the strains applied to fuel cladding during NCT to the strength of Zircaloy-4 cladding enables an assessment of the ability of the cladding to withstand post-storage transportation environments. The data from these tests can also be used to validate finite element models used to predict the behavior of aged, high-burnup fuel under normal conditions of transport.

The data needed to help predict whether aged, high-burnup fuel can withstand normal conditions of transport falls in two categories: 1) the loads imposed directly on rods during NCT (the scope of this paper); and 2) the material properties of aged, high-burnup cladding. Fuel rods subjected to high burnups *may* be sufficiently embrittled such that loads applied to the rods during normal transport *could* result in rod failure.

Zircaloy-4 cladding burned to high levels will likely experience an increase in yield strength with a significant decrease in ductility. Brittle fracture of high-burnup Zircaloy-4 could occur at applied stresses approaching the yield strength of the material. High-burnup Zircaloy-4 may also be below the ductile-to-brittle transition temperature at temperatures associated with long-term dry storage and subsequent transport of used fuel. This implies that the alloy will be at its "lower shelf" and susceptible to brittle fracture. Unirradiated and low-burnup Zircaloy-4 likely exhibits ductility at stress levels beyond the yield strength and is less susceptible to brittle fracture.

The margin of safety between the applied loads on fuel rods and the material properties of the high-burnup rods has not been quantified. So, one relevant question is,

Are the stresses and strains applied to the fuel rods during normal conditions of transport less than the yield strength of the Zircaloy-4?

Data from this test
strains / stresses$_{\text{normal transport}}$

Data from other UFD programs
< properties$_{\text{cladding}}$?

OBJECTIVES OF THE TEST

The objectives of this test program were to:

- Simulate over-the-road tests on a full-scale surrogate fuel assembly by applying loadings to fuel cladding that would be experienced during normal conditions of truck transport.
- Instrument the cladding to measure accelerations and strains imposed by the mechanical loadings resulting from the normal condition of transport vibrations and shocks.
- Provide a data point– applied strain/stress$_{\text{normal transport}}$ - related to the issue of the margin of safety to understand if there is an immediate concern about the ability for aged/high burnup UNF to withstand normal conditions of transport.

BASIS OF TEST

The *ideal test* would be to place an *irradiated fuel assembly* in an *actual cask* and do *over-the-road/rail tests* to measure the vibrational and shock response of the rods to the transport conditions. But, performing such a test with an irradiated assembly would be costly and instrumenting high-burnup cladding would result in high personnel radiation exposures.

An alternative solution is to use an *unirradiated assembly* in an *actual cask*. However, no rail casks are available and the available truck casks have internal contamination because they have all been in reactor pools.
Due to these conditions, the practical alternative was to place an unirradiated fuel assembly on a shaker and subject the assembly to vibrations and shocks simulating normal transport via a truck cask. Three of the surrogate fuel rods in the assembly were Zircaloy-4 – these rods were instrumented- and the remaining tubes were copper. All the tubes contained a lead rod which simulated the UO_2.
Compromises were required in the test design. Table 1 identifies components of an ideal test, constraints to these components, and the compromises made to develop the final test configuration.

Table 1. Constraints and compromises for the shaker assembly test

Ideal Experimental Design	Constraint	Compromise Solution for Test	Comments
Use actual cask	• Available truck casks contaminated • Rail casks unavailable	**Simulate truck transport with a shaker**	Applicable shock/vibration data available from NUREG/CR-0128
Use actual PWR assembly	Use of an irradiated assembly not feasible	**PWR assembly was available**	
Use zirconium alloy rods	Limited number of Zircaloy-4 rods available	• **Use copper alloy tubes for most assembly locations** • **Use Zircaloy-4 rods for those rods to be instrumented**	Among many materials evaluated for surrogates for Zircaloy-4 and UO_2, copper and lead had best combination of material properties (elastic modulus and density, respectively), availability, and cost
Use UO_2 pellets in rods	UO_2 pellets unavailable	**Use lead rods as surrogate**	
Rods have same material properties as used in an actual assembly	• Limited number of Zircaloy-4 rods available • UO_2 pellets unavailable	• **Adjust wall thickness of copper tubes so that $EI_{Cu} \approx EI_{Zircaloy-4}$** • **Adjust amount of lead in tubes so total assembly weight is that of an actual assembly**	

Ideal Experimental Design	Constraint	Compromise Solution for Test	Comments
Assembly is in an actual basket which is within a cask	Actual basket unavailable	**Construct a basket to contain assembly**	
Basket within a truck cask has some freedom of motion	Experimentally unviable to allow basket to move shaker due to shaker control constraints	**Attach basket to shaker to prevent motion**	
Assembly in basket has freedom of motion	None	**Fuel assembly allowed same freedom of motion as an assembly within an actual NAC-LWT PWR basket**	Within the basket, the assembly had 0.45 in. (1.14 cm) clearance at the top and 0.225 in. (0.57 cm) along the sides
Assembly subjected to actual truck transport environment	Truck cask unavailable	**Derive inputs for shaker from truck vibration/shock data**	• Vibration data and shaker inputs ranged from 5 Hz to 2,000 Hz • Shock data ranges from 0.5 Hz to 420 Hz. Shaker inputs for shock ranged from 4 Hz to 600 Hz
Basket/ assembly within an actual truck cask	Truck cask unavailable	• **Basket constructed to conform to material (aluminum), weight, and internal dimensions of NAC-LWT PWR basket** • **Basket affixed to shaker**	
Instrument assembly and basket (accelerometers and strain gages)	None	• **Apply expert judgment and analyses to define location of instruments** • **Instrument selected rods**	• All rods are expected to respond in a similar manner (per analyses) • Used 16 strain gages and 25 accelerometers

TEST PARAMETERS

Instrumentation

Zircaloy-4 rods were placed within the assembly at the top-middle rod location; a top-side location; and the bottom-side location below the top-side Zircaloy-4 rod. Copper tubes were placed at the other locations. Pre-test modeling [6] indicated that all the rods should experience similar loading and so the location of the instrumented rods was arbitrary. Instrumentation was placed at various locations on these three rods at the midpoint between selected spacer grid supports and adjacent to the spacer grids to provide a representative profile of the loading on the rods. Strain gages were placed on the cladding to measure strains during the tests. Accelerometers were placed at strategic locations on the shaker, basket, assembly spacer grids, and selected rods (Figure 1). The tests employed 16 strain gages and 25 accelerometers.

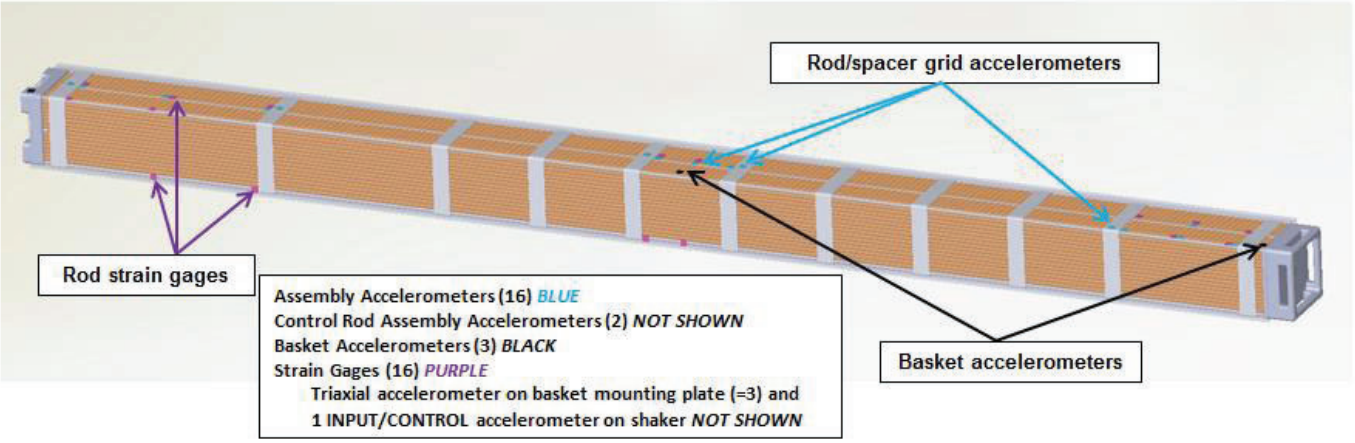

Figure 1. Location of instrumentation on assembly/basket for shaker tests. There were three Zircaloy-4/lead rods and 261 copper/lead rods.

Figure 2 shows the location of the Zircaloy-4 rods which were instrumented and instrumentation on the rods in the actual assembly.

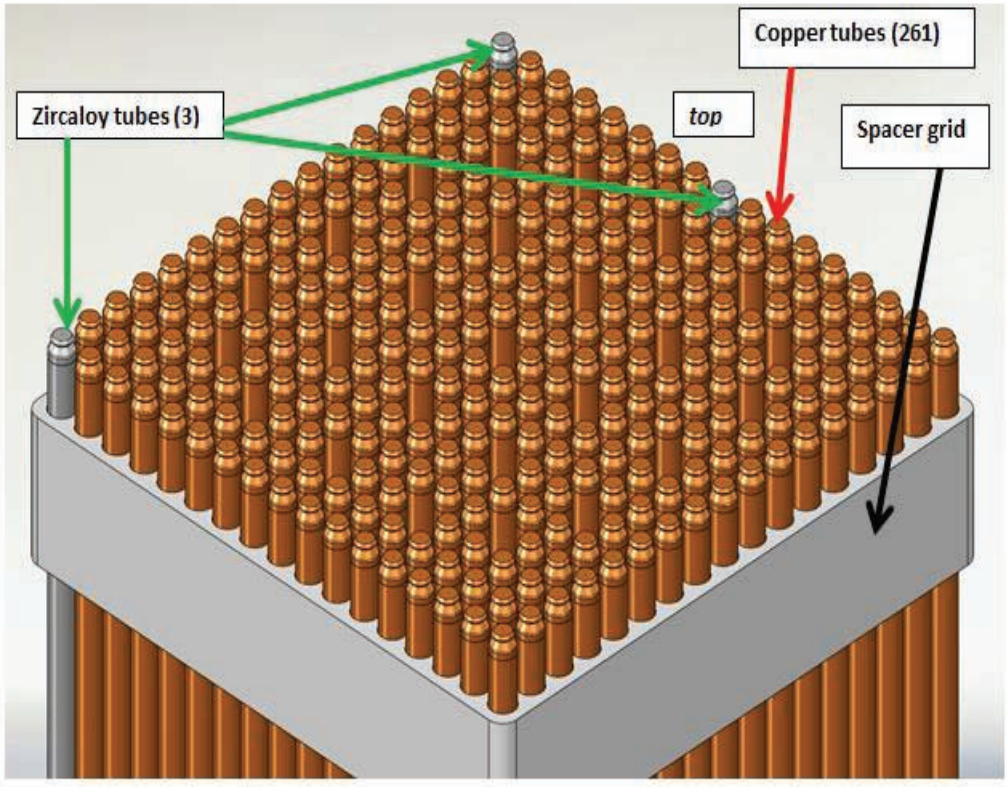

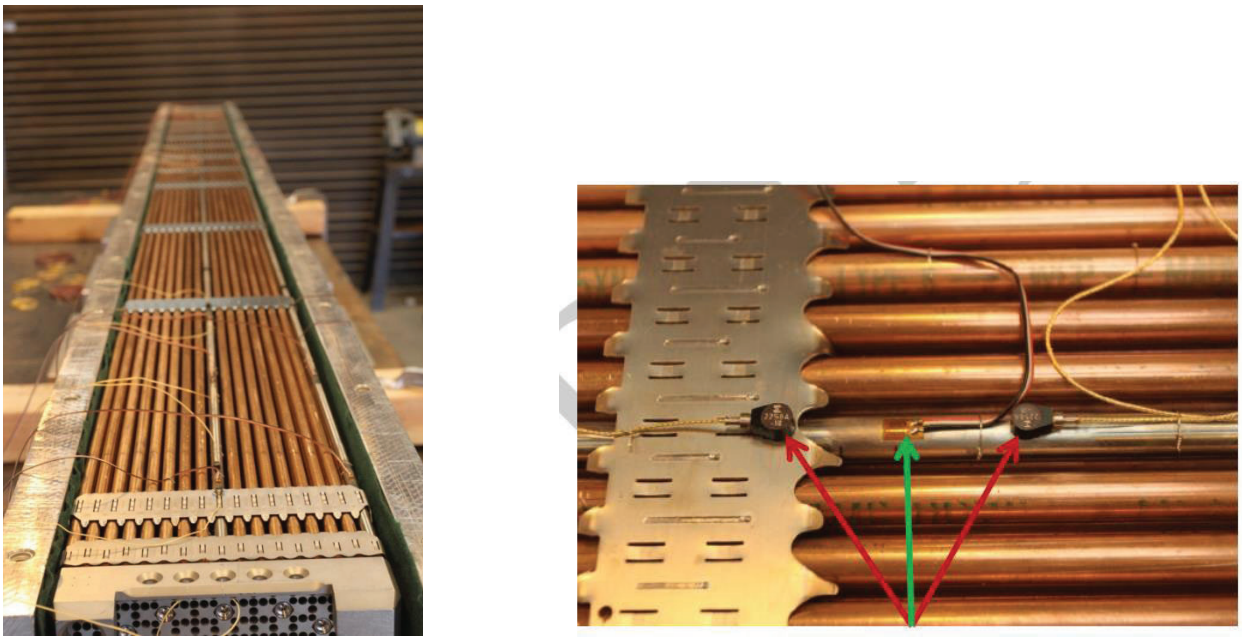

Figure 2. Diagram showing the Zircaloy-4 rods instrumented for the tests (top) and instrumentation on the actual assembly (bottom). The Zircaloy-4 rod shows as "silver" in comparison to the copper rods.

Shaker

The shaker used for the tests was a MB Dynamics C220 base-isolated electrodynamic shaker system located in the Sandia Experimental Environmental Simulation Organization's Vibration and Acoustics Laboratory. The shaker has a 4-ft (1.22 m) shaker head diameter. A 4-ft by 5-ft (1.22 x 1.52 m) expander head was mounted onto the shaker head (Figure 3). Capabilities of the shaker include: 10-2000 Hz sine/random, 30000 lbs. (13608 kg) force, 86 g peak, 45 in./sec (114 cm/sec) velocity, and 2-in. (5.1 cm) peak-to-peak displacement.

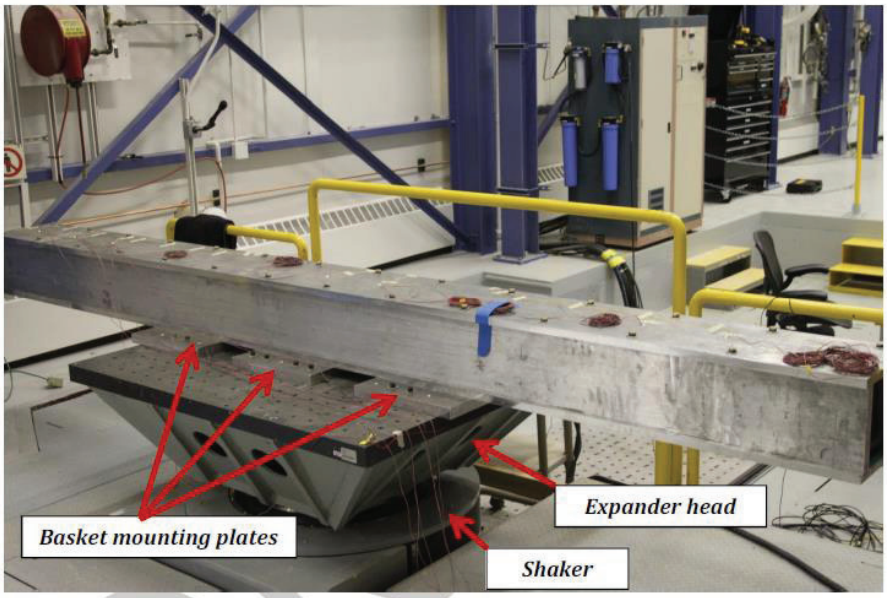

Figure 3. Basket containing assembly on the shaker.

Test input specifications

Input for the shaker was derived from data in "Shock and Vibration Environments for a Large Shipping Container During Truck Transport (Part II)", NUREG/CR-0128 (SAND Report 78-0337), 1978 [4]. Key details from NUREG/CR-0128 are:

- Vibration and shock data were measured by accelerometers over a 700-mile (1127 km) journey. Two tests, two casks.
- 56000-pound (25401 kg) cask and 44000-pound (19958 kg) cask.
- Measurements were taken on the external body of the casks.
- Speeds ranged from 0 to 55 mph (0 to 89 km/h).

Using the most conservative data from this report – the vertical direction - the shaker simulated the vibration and shock experienced by the casks during normal transport. Figure 4 shows the random vibration test specification input to the shaker control system and applied to the basket/assembly. Table 2 lists the corresponding breakpoints.

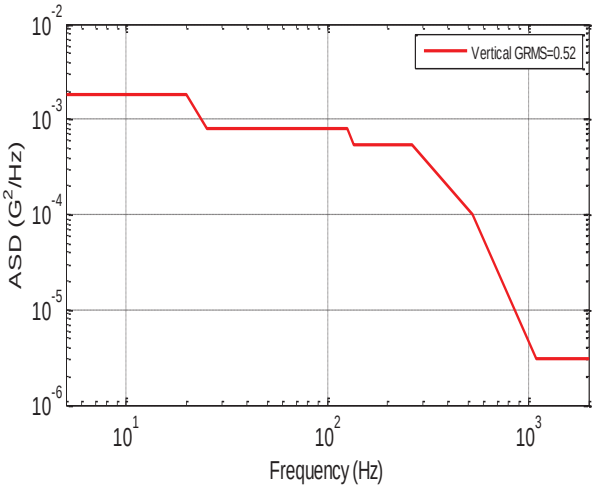

Figure 4. Random vibration test specification

Table 2. Vibration Breakpoints

Frequency (Hz)	(g^2/Hz)
5	1.8e−3
20	1.8e−3
25	8.0e−4
125	8.0e−4
135	5.5e−4
265	5.5e−4
530	1.0e−4
1,100	3.0e−6
2,000	3.0e−6

Figure 5 shows the recommended shock test specification. Table 3 lists the corresponding breakpoints.

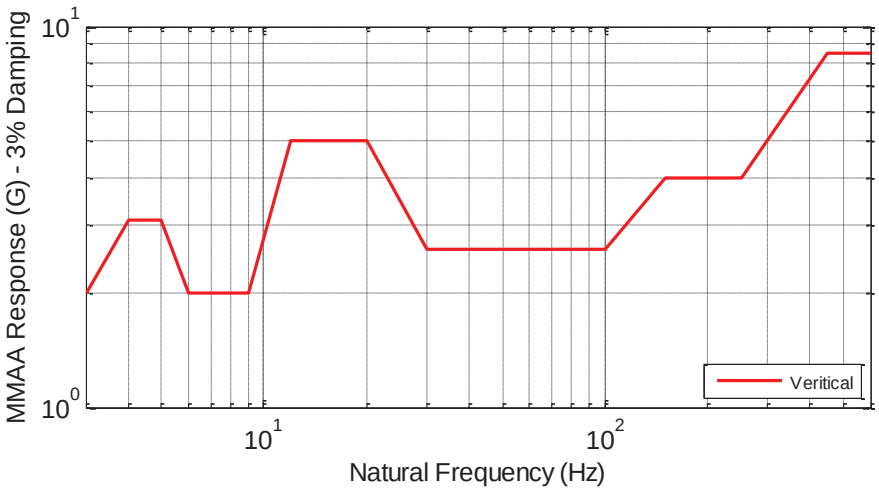

Figure 5. Recommended Shock Test Specification.

Table 3. Reference Shock Breakpoints

Frequency (Hz)	g
3	2
4	3.1
5	3.1
6	2
9	2
12	5
20	5
30	2.6
100	2.6
150	4
250	4
450	8.5
600	8.5

Test sequence

A total of 11 valid tests, six duplicative vibration tests and five duplicative shock tests, of the basket/assembly unit were performed on the shaker April 30 and May 1, 2013. Frequencies input for the shock tests were limited to a lower bound of 4 Hz.

RESULTS

A segment of the time-history data for a shock and vibration test in units of micro-strain *v*. time for all of the strain gages are shown in Figure 6. Note the magnitude of the peak strains.

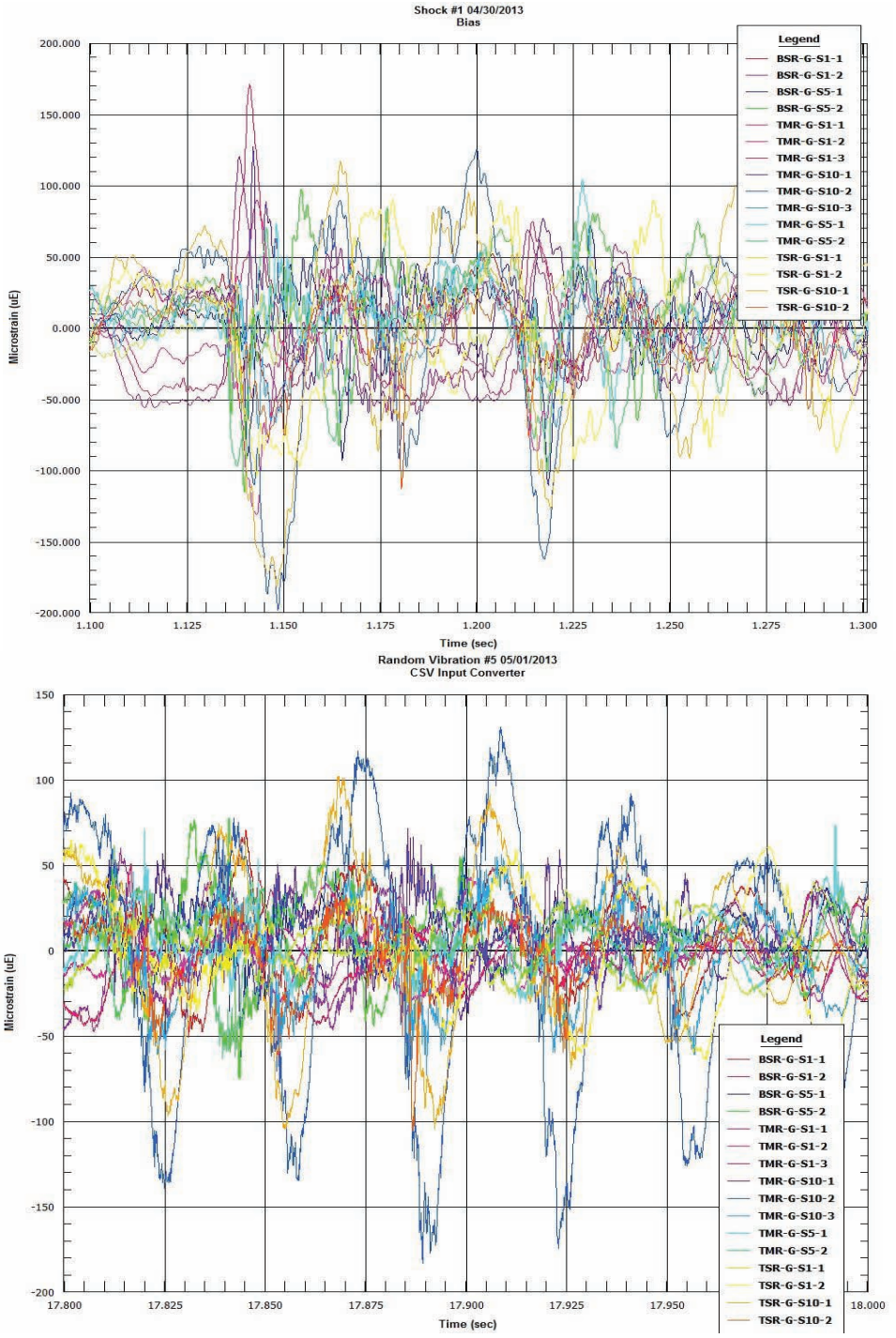

Figure 6. Micro-strain *v.* time for a shock and vibration test for all strain gages

Magnitude of Strains

Tables 4 and 5 present micro-strain and acceleration data recorded for each instrument. There was very little difference between strains measured on the rods due to shock loadings or vibration loads.

Table 4. Strains measured at each strain gage for a shock test

Maximum Strains on Zircaloy Fuel Rods, Shock Test #1			
Rod Location	**Assembly Span**	**Position on Span**	**Maximum Strain (μin./in.)**
Top-middle rod	Bottom-end	Adjacent to spacer grid	90
Top-middle rod	Bottom-end	Mid-span	131
Top-middle rod	Bottom-end	Adjacent to spacer grid	171
Top-middle rod	Mid-assembly	Adjacent to spacer grid	104
Top-middle rod	Mid-assembly	Mid-span	97
Top-middle rod	Top-end	Adjacent to spacer grid	127
Top-middle rod	Top-end	Mid-span	199
Top-middle rod	Top-end	Adjacent to spacer grid	70
Top-side rod	Bottom-end	Adjacent to spacer grid	54
Top-side rod	Bottom-end	Mid-span	107
Top-side rod	Top-end	Mid-span	117
Top-side rod	Top-end	Adjacent to spacer grid	113
Bottom-side rod	Bottom-end	Mid-span	62
Bottom-side rod	Bottom-end	Adjacent to spacer grid	121
Bottom-side rod	Mid-assembly	Adjacent to spacer grid	110
Bottom-side rod	Mid-assembly	Mid-span	115
		Average of All Strain Gages	**112**
		Average Top-middle Rod	124
		Average Top-side Rod	98
		Average Bottom-side Rod	102
		Average Bottom-end Span	105
		Average Mid-assembly Span	107
		Average Top-end Span	125
		Average Mid span	118
		Average Adjacent to Spacer Grid	107

Table 5. Strains measured at each strain gage for a vibration test

Maximum Strains, Average Strains ($\mu\varepsilon_{RMS}$), and Average Peak Strains ($\mu\varepsilon_{peak}$) on Zircaloy Fuel Rods Random Vibration Test #5					
Rod Location	**Span**	**Position on Span**	**Maximum Strain (μin./in.)**	**Average ($\mu\varepsilon_{RMS}$) (μin./in.)**	**Average ($\mu\varepsilon_{peak}$) (μin./in.)**
Top-middle	Bottom-end	Adjacent to spacer grid	70	19	27
Top-middle	Bottom-end	Mid-span	75	21	30
Top-middle	Bottom-end	Adjacent to spacer grid	81	19	27
Top-middle	Mid-assembly	Adjacent to spacer grid	145	15	21
Top-middle	Mid-assembly	Mid-span	80	19	27
Top-middle	Top-end	Adjacent to spacer grid	98	14	20
Top-middle	Top-end	Mid-span	183	42	59
Top-middle	Top-end	Adjacent to spacer grid	74	16	23
Top-side	Bottom-end	Adjacent to spacer grid	60	13	18
Top-side	Bottom-end	Mid-span	128	26	37
Top-side	Top-end	Mid-span	153	41	58
Top-side	Top-end	Adjacent to spacer grid	113	15	21
Bottom-side	Bottom-end	Mid-span	74	17	24
Bottom-side	Bottom-end	Adjacent to spacer grid	71	19	27
Bottom-side	Mid-assembly	Adjacent to spacer grid	106	11	16
Bottom-side	Mid-assembly	Mid-span	92	13	18
		Average All Strain Gages	**100**	**20**	**28**
		Average Top-middle Rod	101	21	30
		Average Top-side Rod	114	24	34
		Average Bottom-side Rod	86	15	21
		Average Bottom-end Span	80	19	27
		Average Mid-assembly Span	106	15	21
		Average Top-end Span	124	26	37
		Average Mid-span	112	26	37
		Average Adjacent to Spacer Grid	91	16	23

The maximum strain on a fuel rod measured during three shock tests listed in Table 6 was 213 µin./in. (213 µm/m) which was at the mid-span of Span 10 of the top-middle rod during Shock Test #2. Span 10 is one of the longer spans located at the top-nozzle end of the assembly.
For Shock Tests #1, #2, and #5 the absolute value of the average maximum micro-strain for all the strain gages was 99 µin./in. (99 µm/m).
The maximum strain on a fuel rod measured during three vibration tests listed in Table 6 was 207 µin./in. (207 µm/m) which was again at the mid-span of Span 10 of the top-middle rod during Random Vibration Test #4. For Random Vibration Tests #4, #5, and #6 the absolute value of the average maximum micro-strain for all the strain gages was 91 µin./in. (91 µm/m).
The stresses corresponding to the maximum experimentally measured strains are approximately 3 ksi (20.6 MPa) as shown in Figure 7. The figure is a plot of the elastic portion of the stress-strain curves for unirradiated and low- and high-burnup Zircaloy-4. The figure indicates just how low the magnitude of the strains and corresponding stresses were on the rods relative to the elastic limit of unirradiated and irradiated Zircaloy-4.
The results suggest that failure of the rods during NCT is unlikely due to a strain- or stress-based failure mechanism. The applied strains on the rods and the corresponding applied stresses may be too low relative to the strength of the cladding to cause failure in the absence of cracks. Further work is underway in other DOE programs to assess Zircaloy-4 performance based on inelastic, brittle fracture material property conditions.

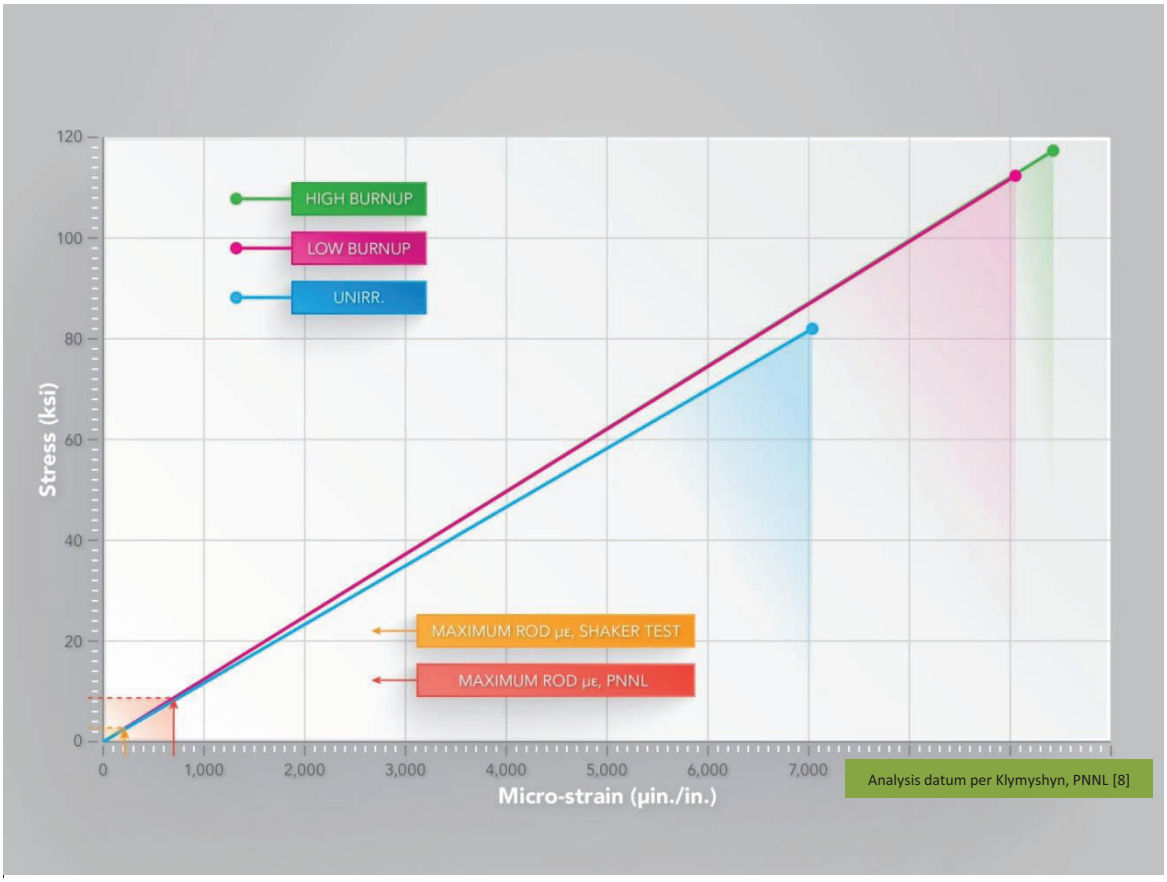

Figure 7. Elastic portion of stress—strain curve for Zircaloy-4 [7], unirradiated, 100°F; low burnup, 250°F; and high burnup, 250°F.

Figure 8 indicates that the desired inputs for the shock and vibration tests were realized as measured by input/control accelerometer on the shaker.

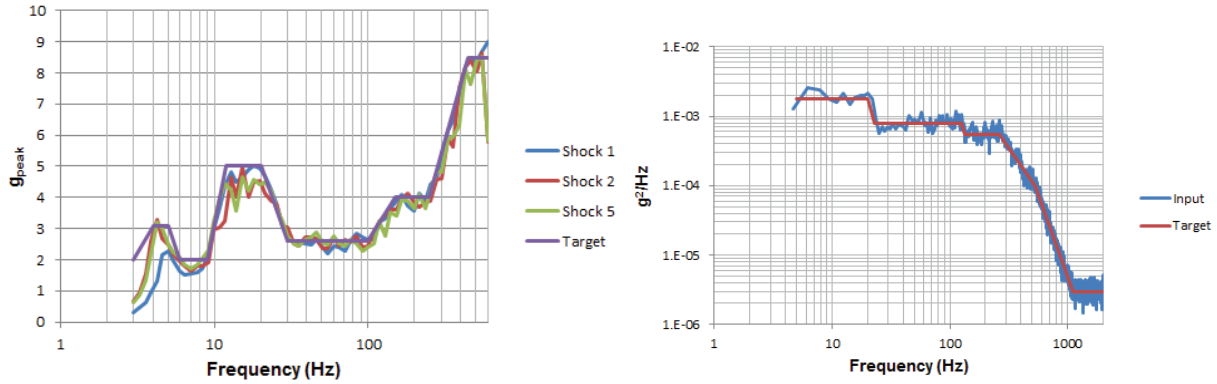

Figure 8. Input/control accelerometer response for shock (left), g *v*. Hz, and vibration (right), g^2/Hz *v*. Hz, relative to the desired target spectra.

Figure 9 show the acceleration power spectral density, g^2/Hz *v*. Hz, of the assembly, as measured on the accelerometers on the central control rod, (top) and the basket (bottom).

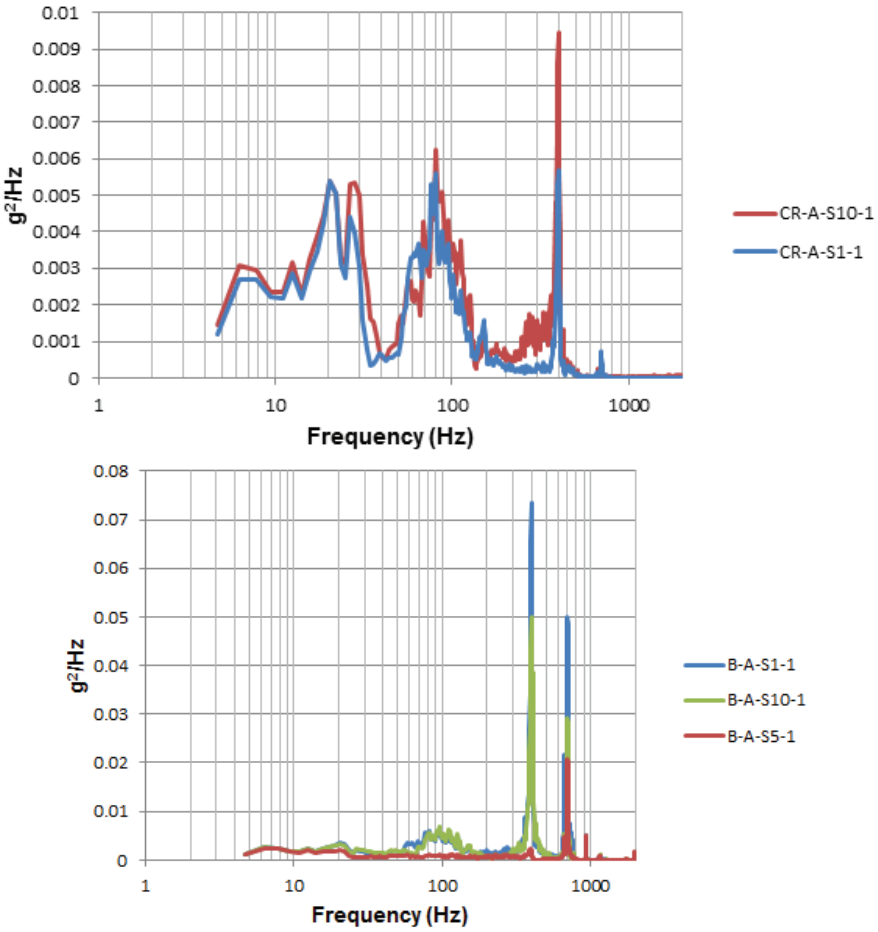

Figure 9. Control rod and basket acceleration power spectral density, g^2/Hz *v*. Hz.

Figure 10 shows the response of the top-middle Zircaloy-4 rod at the long span between spacer grids adjacent to the bottom end of the assembly for a vibration test.

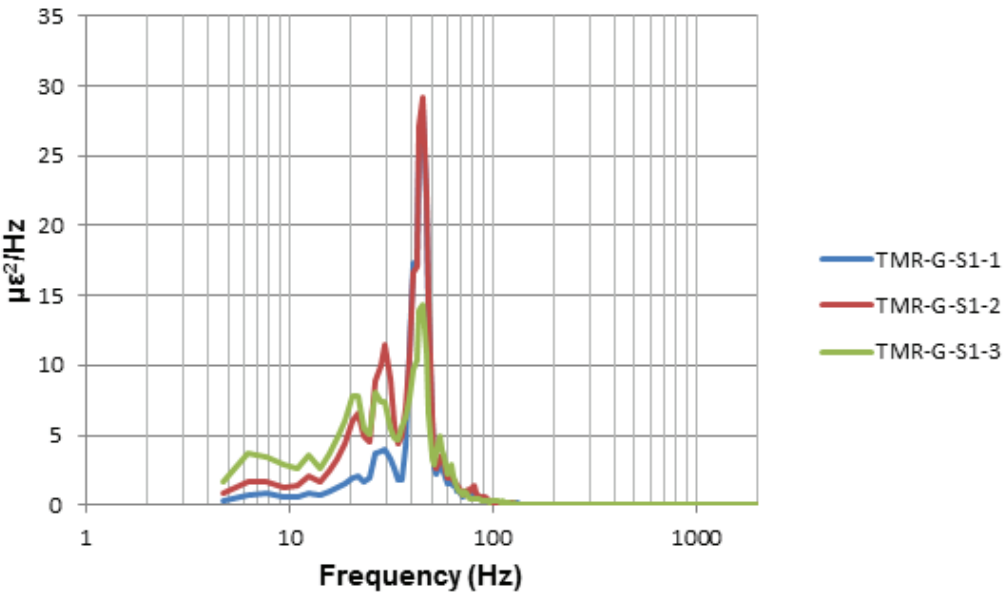

Figure 10. Power spectral density, $\mu\varepsilon^2$ *v.* Hz, for the top-middle Zircaloy- 4 during a vibration test

Comparison of Duplicative Test Data

Table 6 compares the maximum strains measured at all locations for Shock Tests #1, #2, and #5 and Random Vibration Tests #4, #5, and #6. This comparison confirms that test results were nearly identical from test to test. For example, the absolute values of the maximum micro-strains measured by the strain gage denoted TM-10-2 for Shock Tests #1, #2, and #5 were 199 με, 213 με, and 184 με; the absolute values of the maximum micro-strains measured by the strain gage denoted TM-10-2 for Random Vibration Tests #4, #5, and #6 were 207 με, 183 με, and 172 με.

Table 6. Comparison of strains for duplicative vibration and shock tests

Maximum Strains (μin./in.), Each Strain Gage, Duplicative Tests												
Gage	Vibration #4		Vibration #5		Vibration #6		Shock #1		Shock #2		Shock #5	
	Max	Min	Max	Min	Max	Min	Max	Min	Max	Min	Max	Min
TM-1-1	69	−60	70	−59	65	−56	90	−46	91	−49	64	−43
TM-1-2	69	−74	67	−75	64	−77	48	−130	56	−119	63	−119
TM-1-3	73	−64	81	−65	71	−57	172	−53	138	−84	148	−75
TM-5-1	156	−66	145	−57	145	−61	104	−64	90	−83	114	−61
TM-5-2	61	−82	70	−80	64	−97	75	−97	99	−88	89	−119
TM-10-1	90	−55	98	−48	83	−47	127	−66	91	−62	107	−77
TM-10-2	138	−207	131	−183	121	−172	126	−199	169	−213	101	−184
TM-10-3	74	−89	67	−74	62	−76	53	−70	69	−71	42	−80
TS-1-1	55	−41	60	−40	70	−45	53	−36	71	−42	85	−67
TS-1-2	97	−122	89	−128	93	−105	107	−110	114	−139	134	−150
TS-10-1	110	−143	113	−153	101	−146	118	−181	130	−153	149	−198
TS-10-2	45	−113	42	−113	45	−106	35	−112	42	−119	45	−115
BS-1-1	67	−69	74	−61	46	−67	55	−62	74	−70	61	−81
BS-1-2	68	−72	71	−58	62	−56	121	−60	116	−74	85	−75
BS-5-1	65	−108	106	−94	70	−97	71	−111	56	−102	60	−120
BS-5-2	94	−98	90	−92	94	−105	97	−115	88	−111	94	−91

Fracture Mechanics Analysis Based on Stresses from Test Data and Analyses

Cladding could fail via a fracture mechanics-based criterion. Brittle fracture can occur at any stress below the yield limit in cladding containing preexisting flaws or flaws that develop under fatigue loading. In the presence of a crack in the cladding of sufficient size, fracture could occur at relatively low stresses.

An evaluation of the stresses required to cause fracture in the presence of cracks in high-burnup cladding of various sizes was made. These evaluations required an estimate of the fracture toughness, K_{Ic}, of high-burnup Zircaloy-4. Data for the fracture toughness of Zircaloys is discussed in References [7] and [9]. The data suggests a degradation of the fracture toughness of high-burnup Zircaloy-4.

In order to calculate the stress or crack size required to cause fracture of the cladding, equations relating the applied stress intensity, K_I, to the crack size and the applied stress are used. When the applied stress intensity, K_I, exceeds the fracture toughness, K_{Ic}, fracture at the crack tip occurs. A circumferential crack is the most likely to cause fracture in the presence of axial, bending stresses such as those experienced by cladding.

The expression used for the calculations was:

$$K_I = Y\sigma_b\sqrt{(\pi a)}, \text{ where } Y = 1, \sigma_b = \text{applied bending stress [10]}$$

The Zircaloy-4 rods have a wall thickness, t, of 0.0225 inches (0.57 mm). Semi-elliptical circumferential surface cracks with a/2c = 1/6 was assumed, where "a" is the crack depth at the deepest point and "2c" is the length of the crack. The assumed applied stress was 3 ksi (20.6 MPa) which corresponded to the maximum strain measured during the shaker tests. The calculations also assumed partial-through-wall flaws of varying depth, a/t = 0.1, 0.25, and 0.5. Table 7 presents results of the applied stress intensities for the maximum applied stresses tests for a range of crack sizes.

Table 7. Estimated applied stress intensities at the tip of circumferential flaws in the cladding of a fuel rod subjected to the experimentally measured maximum stress, 20.6 MPa

Crack depth/Zircaloy-rod wall thickness	Applied stress intensity at crack tip, (MPa-√m)	Lower bound Zircaloy-4 fracture toughness, (MPa-√m)
0.10	0.3	20 - 30
0.25	0.4	
0.50	0.6	

The calculated applied stress intensities are low relative to the lower bound fracture toughness for Zircaoly-4 and crack depths up to half the clad wall thickness, t; i.e., the fracture toughness of Zircaloy-4 significantly exceeds the applied stress intensities calculated for the stress levels measured for the shaker tests. The resulting implication is that the margin against failure in the presence of a crack on the fuel cladding due to a fracture mechanics-based failure mechanism may be acceptable for the stresses measured by the shaker tests that simulate those expected during normal conditions of transport. The measured strains are very low; it would take a significant preexisting flaw in cladding, and/or significantly degraded fracture toughness, and/or large numbers of cycles under these strains for these strains to be of real concern. This issue should be more thoroughly examined, however, particularly by means of generating additional fracture toughness data on high-burnup Zircaloy-4 and assessments of the sizes of potential cracks in cladding.

CONCLUSION AND FUTURE PLANS

The strains measured in the shaker test program were in the micro-strain levels – well below the elastic limit for either unirradiated or irradiated Zircaloy-4.

Based upon the test results, which simulated normal vibration and shock conditions of truck transport, strain- or stress-based failure of fuel rods during normal transport seems unlikely. Additional testing – shaker tests and high burnup Zircaloy rod characterization – and additional finite elements analyses are recommended.

Future plans for measuring strains on an assembly are to 1) perform tests on the assembly/basket test unit on the Sandia shaker using rail vibration and shock inputs; 2) perform tests on the assembly/basket test unit on a seismic shaker down to 1 - 2 Hz using truck and rail vibration and shock inputs; and 3) instrument an assembly for actual over-the-road testing.

ACKNOWLEDGMENTS

The authors acknowledge John Orchard and Ned Larson of the US Department of Energy; Gordon Bjorkman of the US Nuclear Regulatory Commission; Harold Adkins, Brady Hanson, and Nicholas Klymyshyn of Pacific Northwest National Laboratory; and Robert Wauneka, Greg Koenig, Melissa C de Baca, Jerome Cap, Ron Coleman, Gregg Flores, John Bignell, Remi Dingreville, Sam Durbin, and Sylvia Saltzstein, all of Sandia National Laboratories, for their invaluable technical support, advise, and encouragement.

REFERENCES

[1] Code of Federal Regulations, Title 10, Part 71, "Packaging and Transportation of Radioactive Material."

[2] "Regulations for the Safe Transport of Radioactive Material," Specific Safety Requirements No. SSR-6, International Atomic Energy Agency, 2012.

[3] Standard Review Plan for Transportation Packages for Radioactive Material, NUREG-1609, US Nuclear Regulatory Commission.

[4] Magnuson, Cliff F., "Shock and Vibration Environments for Large Shipping Container During Truck Transport (Part II)," NRC NUREG/CR-0128, May 1978; and Magnuson, Cliff F., "Shock and Vibration Environments for Large Shipping Container During Truck Transport (Part I)," SAND77-1110, September 1977.

[5] Magnuson, C.F., "Shock Environments for Large Transport Containers During Rail-Coupling Operations," Sandia National Laboratories, NUREG/CR-1277, June 1980.

[6] Nicholas Klymyshyn, "Shaker Table Modeling Progress Report," #UFDCST-120927-1, Pacific Northwest National Laboratory, September 2012.

[7] Ken Geelhood and Carl Beyer, "Used Nuclear Fuel Loading and Structural Performance Under Normal Conditions of Transport – Supporting Material Properties and Modeling Inputs," Pacific Northwest National Laboratory, FCRD-UFD-2013-000123, March 2013.

[8] Nicholas Klymyshyn, Scott Sanborn, Harold Adkins, and Brady Hanson, "Fuel Assembly Shaker Test Simulation," FCRD-UFD-2013-000168, Pacific Northwest National Laboratory, May 2013.

[9] Rashid, Y.R., R.O. Montgomery, W.F. Lyons, "Fracture Toughness Data for Zirconium Alloys – Application to Spent Fuel Cladding in Dry Storage," Electric Power Research Institute Technical Progress Report 1001281, January 2001.

[10] FITNET Annex A, "Stress intensity factor (SIF) solutions," *ocw.unican.es/ensenanzas-tecnicas/.../otros.../soluciones_fit__fitnet_.pdf, May 2006.*